

<http://ansinet.com/itj>

ITJ

ISSN 1812-5638

INFORMATION TECHNOLOGY JOURNAL

ANSI*net*

Asian Network for Scientific Information
308 Lasani Town, Sargodha Road, Faisalabad - Pakistan

Robotic Manipulator Parameterized Self-motion Manifold

¹Lin Yong and ²Ge Xinfeng

¹College of Zhijiang, Zhejiang University of Technology, Hangzhou, China

²College of Electrical and Information Engineering, Xuchang University, Xuhang, China

Abstract: The self-motion of redundant robot is analyzed that take the natural coordinates of points as independent motion parameters for the points in redundant robot's workspace, then this method is applied to analyze the self-motion of the 7-DOF (Degree of Freedom) automatic fiber placement robotic manipulator, come to the self-motion manifold of 7-DOF automatic fiber placement robotic manipulator. The self-motion curves of 7-DOF automatic fiber placement robotic manipulator derived by parameterized and numerical methods and were compared; the results show that the parameterized methods used to analyze the self-motion of the redundant robotic manipulator is an effective approach.

Key words: Redundant robotic manipulator, parameterization, self-motion manifold, fiber placement

INTRODUCTION

In the redundant robotic manipulators self-motion manifold researches, for self-motion manifold comprising all configurations and reflecting the robotic end-effector self-motion ability and becomes the hot research in the redundant robotic manipulators kinematics study (Lu, 2007). In the robot control, the inverse kinematics is the basis for realizing motion planning and motion control, all the same for redundant robotic manipulator. Therefore, to achieve redundant, automatic fiber placement robotic manipulator motion planning and motion control, the inverse kinematics must need to solve firstly. In general, the theoretical analysis method for solving the redundant manipulators self-motion is very difficult (Zhang, 2011; Tang *et al.*, 2011); many scholars (Euler, 1989; Lenarcic., 1999; Liégeois, 1977; Salisbury and Craig, 1982; Angeles and Rojas, 1987; Klein and Blaho, 1987) have adopted the numerical method to solve the redundant robotic manipulators inverse kinematics. The algorithms are based on the gradient of the selected function and optimized to solve the inverse kinematics of redundant robotic manipulator. But in the process of striking the function gradient, the inverse kinematics of redundant robotic manipulator solved may not be the global optimal solution for the definition of gradient; therefore the above algorithm can not guarantee the inverse kinematics solution of redundant robotic manipulator is globally optimal solution. The redundant robotic manipulators inverse kinematics solutions are solved by self-motion manifold method, for this topic, domestic and foreign scholars (Chan and Dubry, 1995; Moll and Kavraki, 2004; Burdick, 1989; Zhao *et al.*, 2007,

2009) have put forward many algorithms. But the researches on the self-motion manifolds of the 7-DOF and more robotic manipulators is still relatively little, in this study, a parameterization algorithm is proposed which solve the redundant robotic manipulators self-motion manifolds, this algorithm can solve the redundant robotic manipulators self-motion manifolds.

MATERIALS AND METHODS

Manifold mapping of the redundant robotic manipulators: Redundant robotic manipulators forward kinematics mapping function f is the nonlinear vector function which mapping from the joint coordinate set θ to the end-effector position and orientation set p . From the view point to point, the joint configuration θ is mapped to the end-effector position by mapping function f , namely:

$$p = f(\theta) \quad (1)$$

The joint space of the i th joint is expressed C_i ; n joints (assuming a joint has one DOF) redundant robotic manipulators joint configuration space can be expressed by multiplying n separate joint space C_i :

$$C = C_1 \times C_2 \times \dots \times C_i \times \dots \times C_n$$

The set of all possible joint configurations of C is called the joint space or configuration space and has a simple manifold structure; similarly, all the position and orientation p of the end-effector form the workspace, also has a manifold structure. From the view of the manifold, the configuration space manifold is mangled into

fragments by the direct kinematics map f and then these fragments is distorted, the workspace manifold W is formed by agglutinated these distorted fragments.

A coordinate system is fixed on the end-effector, the robotic manipulator workspace manifold W is the set of the coordinate system all possible position and orientation when the robotic manipulator joints take over all the points in the conformation space C . f as a global restructuring from the configuration space manifold to the workspace manifold, that is:

$$f(\theta): C \rightarrow W \quad (2)$$

take $u \in W$, so the self-motion manifold is corresponded by u can be expressed a set formed by the configuration subspace C_s and maps set F_s , that is:

$$(C_s, F_s) = \{(\theta, f) | f(\theta) = u, u \in W\} \quad (3)$$

Equation 2 is the manifold mapping that the redundant robotic manipulator configuration space to work space, equation 3 is the self-motion manifold that a position and orientation corresponded in the redundant robotic manipulator workspace.

Redundant robotic manipulator parameterized self-motion manifold: Assume $s = n - m$ and called it is relatively redundant DOF (Degree of Freedom), the inverse kinematics solutions $f^{-1}(x)$ are a discrete conformational bounded set for non redundant robotic manipulator, there are up to 16 inverse kinematics solutions for 6R robotic manipulator which has been proven in (Guillemin and Pollack, 1974), f is a smooth function which from the configuration space manifold C to workspace manifold W , so the inverse kinematics solutions must be s -dimensional sub manifold of C for a given position and orientation p . Although the sub manifold preimage is divided into more than one disjointed manifold. Redundant robotic manipulator inverse kinematics can be expressed as the sum of the r -dimensional disjointed manifolds.

$$f^{-1}(p) = \bigcup_i M_i(\Psi) \quad (4)$$

Here:

- n_m = The self-motion number in preimage
- $M_i(\Psi)$ = The i th s -dimensional manifolds in inverse kinematics preimage

When $i \neq j, M_i \cap M_j = \Phi$, Each preimage manifold actually corresponds to a self-motion. Every $M_i(\Psi)$ can be

parameterized by the set of r independent parameters $\Psi = \{\Psi_1, \dots, \Psi_s\}$, r independent parameters $\Psi = \{\Psi_1, \dots, \Psi_s\}$ can be seen as the natural coordinate of the self-motion. For given position and orientation p , the parameter is the only one, the parameter can be change with p changing.

EXAMPLES

7-DOF automated fiber placement robotic manipulator's topology and parameter: The automated fiber placement robotic manipulator is composed by a 6-DOF fiber placement robotic manipulator and a rotational mandrel (Fig. 1). According to the principle of equivalence movement: mandrel coordinate system is fixed with the base coordinate system, a virtual revolute joint linked the base and the mandrel together, Rotational mandrel is equivalent to the robotic manipulator's rotation around the base. So the fiber placement robotic manipulator with 6-DOF and the mandrel with 1-DOF becomes a 7-DOF redundant robotic manipulator. According to D-H method (Denavit and Hartenberg, 1995), the coordinate system is established (Fig. 2). Which, $X_m Y_m Z_m$ is the mandrel coordinate system; x, y, z is the end-effector coordinate, D-H parameters as shown in Table 1.

7-DOF automated fiber placement robotic manipulator's self-motion manifold curve: According to the principle of equivalence motion, 7-DOF automated fiber placement robotic manipulator can be modeled as a revolute joints formed by 4 anthropomorphic manipulator and a manipulator formed by the three prismatic joint. The 3 prismatic joints determined the size of the workspace, 4 revolute joints determined the orientation. The automated fiber placement robotic manipulator self-motion manifold is the curve in the workspace by the 3 prismatic joint determined, so the self-motion manifolds can be found by analyzing the anthropomorphic manipulator comprised by 4 revolute joints. The anthropomorphic manipulator structure figure comprised by 4 revolute joints is shown in Fig. 3. The former 3 joint $\theta_5, \theta_6, \theta_7$ intersect at one point, called should, the fourth joint called elbow. The up arm length is a_6 , the forearm length is a_3 .

Assume the main task is that the end-effector would track a series of circles in the Cartesian space, the orientation self-motion including the rotation that the elbow center rotating around the shoulder centers and the end-effector axis r . It can be observed from the Fig. 3, there are two different kinematics patterns (Fig. 3a, b). The difference between these two modes there is an intersection or not between the circle generated by the elbow rotating and the x -axis (the first joint axis). When

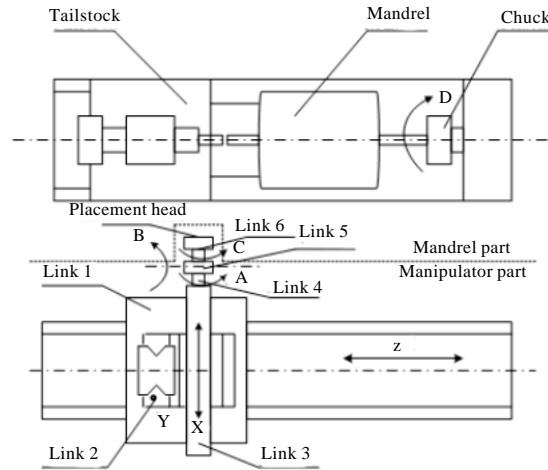


Fig. 1: Automated fibre placement robotic manipulator's structure

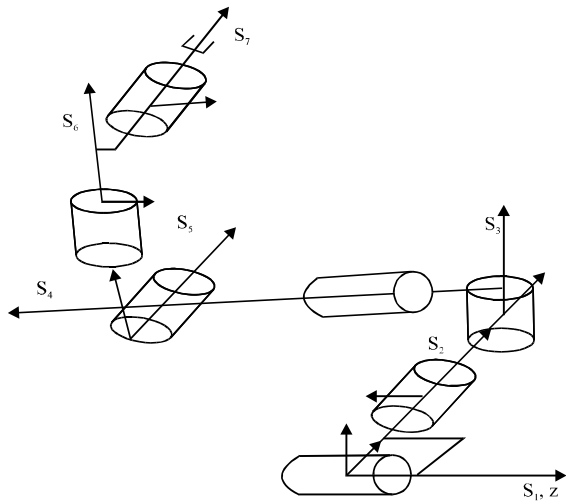


Fig. 2: Automated fibre placement robotic manipulator's topology

Table 1: Parameters of the automated fiber placement robotic manipulator

Linki	α_{i-1} (mm)	α_{i-1} (°)	d_i (mm)	θ_i (°)	Range of each joint
1	α_0	0	0	θ_1	-180~180
2	0	0	d_2	0	-150~150
3	0	90	d_3	-90	-110~110
4	α_3	90	d_4	0	-100~100
5	0	0	c	θ_5	-90~90
6	0	90	0	θ_6	-110~110
7	0	-90	0	θ_7	-260~260

the anthropomorphic manipulator moves along the axis r , the self-motion switch between two different modes. When the anthropomorphic manipulator is fully extended ($r \approx r_{max} = a_0 + a_3$), the self-motion is in the first mode (except for $r = x$). As r decreases, the self-motion would transform from the first mode to the

second mode with r decreasing continuously ($r \approx r_{min} = \|a_0 - a_3\|$), the self-motion remained at the second mode. The anthropomorphic manipulator self-motion curve is shown in Fig. 4 (part from motion curve) corresponding to the different effective distance r ($r_{min} < r < r_{max}$).

The end-effector position can be expressed as follows:

$$r = (x \ y \ z)^T = r_1 + r_2$$

Where:

$$r_1 = a_3 \begin{pmatrix} -\sin \theta_6 & \sin \theta_5 \cos \theta_6 & -\cos \theta_5 \cos \theta_6 \end{pmatrix}^T$$

$$r_2 = a_0 \begin{pmatrix} \cos \theta_1 \cos \theta_2 \cos \theta_6 \\ (\sin \theta_3 \sin \theta_6 \cos \theta_7 + \cos \theta_3 \sin \theta_7) \cos \theta_1 + \sin \theta_1 \sin \theta_3 \cos \theta_6 \\ (-\cos \theta_3 \sin \theta_6 \cos \theta_7 + \sin \theta_3 \sin \theta_7) \cos \theta_1 - \sin \theta_1 \cos \theta_3 \cos \theta_6 \end{pmatrix}$$

figures in the anthropomorphic manipulator $(\theta_1, \theta_5, \theta_6, \theta_7)$, $(\theta_1, \theta_5, \theta_6, \theta_7')$, $(\theta_1, \theta_5', \theta_6, \theta_7')$, $(\theta_1, \theta_5', \theta_6', \theta_7)$, $(\theta_1', \theta_5, \theta_6, \theta_7)$, $(\theta_1', \theta_5, \theta_6', \theta_7)$, $(\theta_1', \theta_5', \theta_6, \theta_7)$ and $(\theta_1, \theta_5, \theta_6, \theta_7)$.

RESULTS

In order to verify the self-motion manifold solved, the robotic manipulator winding S-shaped inlet mandrel is an example. Figure 5 is the desired trajectory of the end-effector on mandrel, Fig. 6 is simulating trajectory of the end-effector on mandrel according to Fig. 5.

Compared Fig. 5 and 6, the simulating trajectory and the desired trajectory are fairly consistent, that

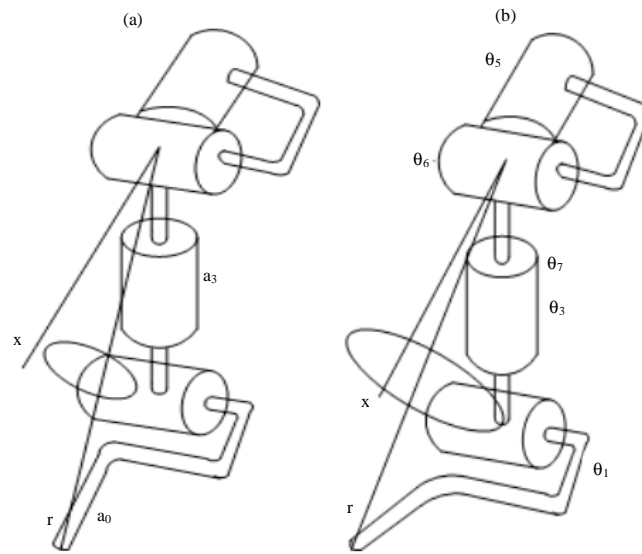


Fig. 3(a-b): Schematic figure of the anthropomorphic manipulator contain 4 revolute joints (a) No intersection between the end-effector motion and the joint axes 1 and (b) There is an intersection between the end-effector motion and the joint axes 1

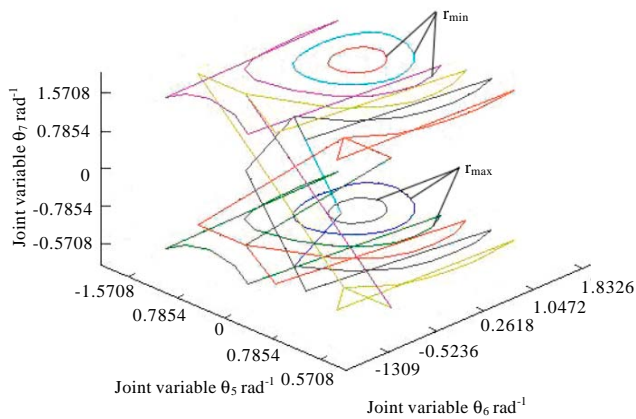


Fig. 4: Anthropomorphic manipulator self-motion curve

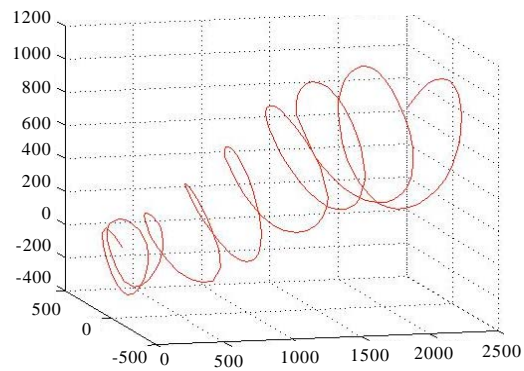


Fig. 5: End-effector desired trajectory

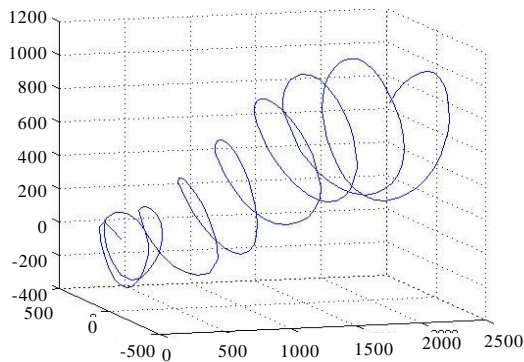


Fig. 6: End-effector simulating trajectory

is to say the self-motion manifold obtained is correctly and applicable.

CONCLUSION

- The method that analyzing the self-motion of redundant robotic manipulator is proposed, by parameterized the robot joint coordinates and derived the redundant robotic manipulator's self-motion curve
- The 7-DOF automated fiber placement robotic manipulator is set as an example, the self-motion manifolds are analyzed and the conclusion is drawn that the robotic self-motion curve is the periodic function about joint coordinate

ACKNOWLEDGMENT

This study is supported by Natural Science Project of Zhejiang Provincial Department (Y201018585).

REFERENCES

Angeles, J. and A.A. Rojas, 1987. Manipulator inverse kinematics via condition number minimization and constitution. *Int. J. Robotics Automation*, 2: 61-69.

Burdick, J.W., 1989. On the inverse kinematics of redundant manipulators: Characterization of the self-motion manifolds. *Proceedings of the IEEE International Conference on Robotics and Automation*, May 14-19, 1989, Scottsdale, AZ., pp: 264-270.

Chan, T.F. and R.V. Dubey, 1995. A weighted least-norm solution based scheme for avoiding joint limits for redundant joint manipulators. *IEEE Trans. Robotics Automation* 11: 286-292.

Denavit, J. and R.S. Hartenberg, 1955. A kinematic notation for lower-pair mechanisms based on matrices. *Trans. ASME J. Applied Mech.*, 23: 215-221.

Euler, J.A., R.V. Dubey and S.M. Babcock, 1989. Self motion determination based on actuator velocity bounds for redundant manipulators. *J. Robotics Syst.*, 6: 417-425.

Guillemin, V. and A. Pollack, 1974. *Differential Topology*. Prentice-Hall, New Jersey, pp: 25-28.

Klein, C.A. and B.E. Blaho, 1987. Dexterity measures for the design and control of kinematically redundant manipulators. *Int. J. Robot. Res.*, 6: 72-83.

Lenarcic, J., 1999. On the quantification of robot redundancy. *Proceedings of the IEEE Conference on Robotics and Automation*, Volume: 4, May 10-15, 1999, Detroit, Michigan, pp: 3159-3164.

Liegeois, A., 1977. Automatic supervisory control of the configuration and behavior of multibody mechanisms. *IEEE Trans. Syst. Man Cybernetics*, 7: 868-871.

Lu, Z., 2007. *Principle and Application of Redundant Robot*. China Machine Press, China.

Moll, M. and E.E. Kavraki, 2004. Path planning for minimal energy curves of constant length. *Proceedings of the IEEE International Conference on Robotics and Automation*, Volume 3, 26 April-1 May 2004, USA., pp: 2826-2831.

Salisbury, J.K. and J.J. Craig, 1982. Articulated hands: Force control and kinematics issues. *Int. J. Robot. Res.*, 1: 4-17.

Tang, G., T. Mei, W. Liu and B. Li, 2011. Kinematics analysis of motion simulation subsystem for unmanned vehicle. *Chin. J. Mech. Eng.*, 24: 923-934.

Zhang, B., 2011. Joint space trajectory planning for robots under multiple constraints. *Chin. J. Mechanical Eng.*, 47: 13-16.

Zhao, J.W., Z.J. Du and L.N. Sun, 2007. Self-motion manifolds of a 7-DOF redundant robot arm. *Chinese J. Mechanical Eng.*, 43: 132-137.

Zhao, J.W., Y.F. Yao and B. Huang, 2009. Self-motion manifold of a redundant robot with coupled pose. *Mech. Sci. Technol.*, 28: 1012-1017.